

Article

Corrosion Properties in Sodium Chloride Solutions of Al–TiC Composites *in situ* Synthesized by HFIHF

El-Sayed M. Sherif ^{1,2,*}, Hany S. Abdo ^{1,3}, Khalil Abdelrazek Khalil ^{3,4} and Ahmed M. Nabawy ¹

¹ Center of Excellence for Research in Engineering Materials (CEREM), Advanced Manufacturing Institute, King Saud University, P.O. Box 800, Al-Riyadh 11421, Saudi Arabia; E-Mails: habdo@ksu.edu.sa (H.S.A.); ahmed.nabawy@cml.ca (A.M.N.)

² Electrochemistry and Corrosion Laboratory, Department of Physical Chemistry, National Research Centre (NRC), Dokki, Cairo 12622, Egypt

³ Mechanical Design and Materials Department, Faculty of Energy Engineering, Aswan University, Aswan 81521, Egypt; E-Mail: kabdelmawgoud@ksu.edu.sa

⁴ Department of Mechanical Engineering, College of Engineering, King Saud University, P.O. Box 800, Riyadh 11421, Saudi Arabia

* Author to whom correspondence should be addressed; E-Mail: esherif@ksu.edu.sa; Tel.: +96-6-533-203-238; Fax: +96-6-114-670-199.

Academic Editor: Hugo F. Lopez

Received: 6 September 2015 / Accepted: 28 September 2015 / Published: 8 October 2015

Abstract: Al–TiC nanocomposite materials have been prepared by a new *in situ* synthesizing technique. A mixture of aluminum, titanium, and graphite has been prepared using ball milling technique and then melted in a high frequency induction heat furnace (HFIHF) at different sintering temperatures, namely 900, 1100, and 1300 °C. The effect of sintering temperature on the corrosion of the Al–TiC composite in 3.5% NaCl solutions was investigated using cyclic potentiodynamic polarization, chronoamperometric current-time, open-circuit potential, and electrochemical impedance spectroscopy measurements. The surface of the composites after their corrosion in the test solution was investigated using scanning electron microscopy and energy dispersive X-ray analyses. It has been found that all manufactured composites suffer uniform corrosion. All corrosion test techniques were consistent with each other and confirmed clearly that the corrosion resistance of Al composites increased according to their sintering temperature in the following order 900 > 1100 > 1300 °C.

Keywords: Al composites; corrosion; mechanical alloying; polarization; sintering temperature

1. Introduction

Aluminum and its alloys are versatile materials thanks to their excellent properties such as high strength to weight ratio, good machinability, excellent corrosion resistance, acceptable appearance, and being heat-treatable [1–5]. Therefore, they have been widely used in several industrial applications such as electrical conductors, construction material of aircrafts, anode material for alkaline batteries and cathodic protection systems, packages, household appliances, *etc.* [1–5]. The corrosion resistance of aluminum results from the natural oxide film that spontaneously forms on its surface once it is exposed to air. This oxide film is more immune to corrosion than the aluminum itself. While, in harsh environments and corrosive aqueous solutions, the corrosion of aluminum takes place as a result of the environmental attack to the aluminum oxide layer formed on the surface leading to its dissolution either via uniform or pitting corrosion or even through the occurrence of both corrosion forms together [2,4,6].

The corrosion resistance of aluminum and its alloys has been reported to be improved in many ways. This includes modifying the surrounding environments to decrease its corrosiveness action through using powerful corrosion inhibitors [6,7]. Also, by increasing the immunity of aluminum itself via adding more noble alloying elements to aluminum [8–10], reducing the grain size of aluminum [11,12], anodization of aluminum [13,14], and using the appropriate heat treatment parameters [15–18]. The inhibition of aluminum corrosion in 3.5% NaCl solution and Arabian Gulf seawater by 3-amino-5-mercapto-1,2,4-triazole (AMTA) has been investigated [6,7]. It is found that the presence of AMTA molecules inhibits the corrosion of aluminum via its adsorption onto the aluminum surface protecting from being attacked by the surrounding corrosive ions and this effect was found to increase with the increase of AMTA concentration. Moreover, the addition of graphite (Gr) as an alloying element [8,9] was found to affect the corrosion behavior of aluminum, where the presence of Gr up to 3.0 wt. % increases the corrosion rate of aluminum in 3.5% sodium chloride solutions on short immersion periods of time, 40 min. Increasing the immersion time of the aluminum containing Gr to three days decreases the rate of corrosion of aluminum through increasing the resistance of its surface to both pitting and uniform attacks. Adding iron in low percentages, 0.04–0.42 wt. %, to aluminum increases the pitting and uniform corrosion by increasing the oxygen reduction and hydrogen evolution reactions [10]. In this case, the heat treatment was found to cause depletion in the solute content of Al containing Fe matrix, leading to the increase of its anodic reactivity.

The corrosion behavior of aluminum and its alloys was also found to be influenced by refining the size of their grains. The refining of grain size can be achieved in different ways, including high pressure torsion and equal channel angle pressing (ECAP). It has been reported [19–22] that ECAP is one of the most employed methods for producing ultra-fine microstructures of Al alloys. The ECAP technique was also reported to remarkably improve the mechanical properties and increase the corrosion resistance of Al alloys [11,12,23–25]. The aim of the present work was twofold. First, the

manufacturing of Al–TiC composites with chemical composition of 65 wt. % Al, 30 wt. % C, and 5 wt. % Ti, at 900, 1100, and 1300 °C. Second, reporting the effect of the different sintering temperatures on the corrosion behavior of the manufactured composite. The study was carried out using a high energy ball mill to uniformly mix the powders of the alloying elements. A high-frequency induction heat sintering at the named temperatures was also employed to obtain the solid form of the composites. The corrosion behavior was tested in 3.5% NaCl solutions using cyclic polarization, chronoamperometric, electrochemical impedance spectroscopy, and scanning electron microscopy investigations.

2. Experimental Part

2.1. Manufacturing of Al–TiC Composites

Aluminum (Al, 98% purity), titanium (Ti, 98% purity), and graphite (Gr, 99.5% purity) fine powders with micro particle size were purchased from Loba Chemie, India and were used as received. The Al fine powder was mixed with the Gr and Ti powders to get a mixture of 65Al–30C–5Ti in weight percent (wt. %). The powders were uniformly mixed in a high energy ball milling using steel balls with ball-to-powder ratio of 5:1 using a Desktop 220V High Energy Vibratory Ball Mill from Across International Company (Livingston, NJ, USA). The mixture of powders was placed in 80 mL steel jar at 2000 rpm and 30 min mixing time. The mixed powders were sintered in a 10 mm graphite die as shown in Figure 1 using high-frequency induction heat sintering. The sintering process was done under 10 MPa pressure (low pressure sintering) at different temperatures of 900, 1100, and 1300 °C, respectively for 4 min. The compaction and sintering processes were done simultaneously at vacuum level of 1×10^{-3} Torr in order to prevent the grain growth and the oxidation of the surface of the composites. The sintered specimens were finally left to cool down to reach room temperature, then were taken out from the chamber of the furnace via the extraction mechanism shown in Figure 1b.

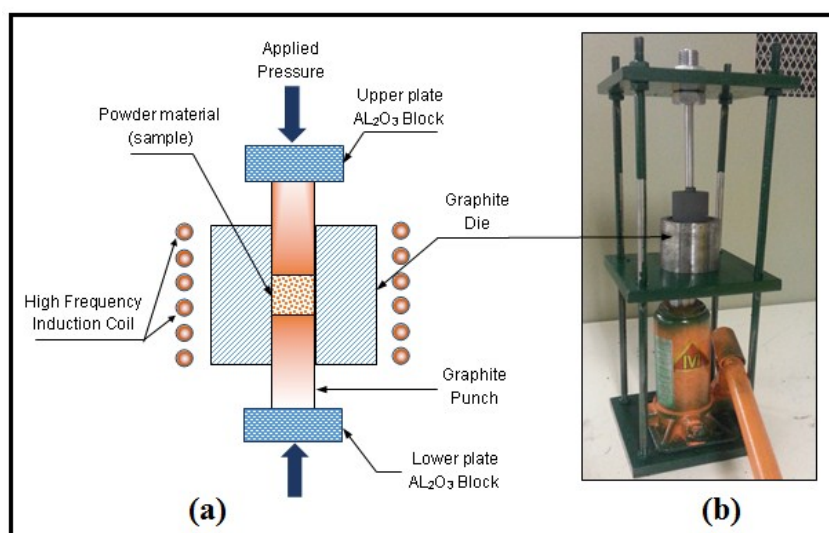


Figure 1. (a) Graphite die during sintering and (b) sample extraction from the graphite die.

2.2. Test Solution and Electrochemical Cell

The pure sodium chloride salt (99%) was obtained from Merck and was used in the preparation of the 3.5 wt. % NaCl solution as received. A conventional electrochemical cell accommodates for 250 cm³ and having a three-electrode configuration was used for the electrochemical measurements. The Al composite, an Ag/AgCl electrode (in saturated KCl solution), and a platinum wire were used as working, reference, and counter electrodes, respectively. The Al electrode was prepared and polished for electrochemical measurements as previously reported [8,26].

2.3. Electrochemical Techniques

The electrochemical measurements were carried out using an Autolab Potentiostat-Galvanostat that was purchased from Metrohm Autolab B.V. (Amsterdam, The Netherlands). The cyclic polarization curves were measured after 1 h immersion in the NaCl solution by scanning the potential from -1.70 V towards the positive direction to 0.0 V at a scan rate of 0.001 V/s against the Ag/AgCl reference electrode. Then, the potential was scanned in the reverse direction at the same scan rate until the end of the run [8,9]. The chronoamperometric experiments were carried out after 1 h immersion in the test solution after which the potential of Al electrodes was kept at a constant potential value of -0.1 V for 1 h. The open-circuit potential measurements were carried out for 24 h. The electrochemical impedance spectra were acquired after 1 h immersion in the chloride solution from the open-circuit potential value [8,9,26]. The frequency was scanned from the range of $100,000$ Hz to 0.1 Hz using an AC wave of ± 5 mV peak-to-peak overlaid on a DC bias potential. The software to collect the impedance data was Powersine software at a rate of 10 points per decade change in frequency [8,9,26]. Each experiment was performed using new portion of the test solution and a fresh electrode surface.

2.4. Surface Characterization

A scanning electron microscope from JEOL (Tokyo, Japan) was used and its images obtained the surface of the Al composites, which were immersed in 3.5 wt. % NaCl solution for 1 h before applying a constant potential value of -0.0 V for 1 h.

3. Results and Discussion

3.1. Cyclic Polarization Experiments

Cyclic potentiodynamic polarization (CPP) measurements were carried out in order to report the corrosion parameters obtained in studying the effect of sintering temperature on the corrosion behavior Al–TiC composites in the chloride test solution. Figure 2 shows the CPP curves obtained in 3.5% NaCl solutions for the Al–TiC composites sintered at (1) 900, (2) 1100, and (3) 1300 °C, respectively. The values of the corrosion parameters obtained from the polarization curves such as cathodic Tafel (β_c) and anodic Tafel (β_a) slopes, the corrosion potential (E_{Corr}), corrosion current density (j_{Corr}), polarization resistance (R_p), and corrosion rate (R_{Corr}) are presented in Table 1. The values of these parameters were obtained as reported in our previous studies [8,9].

Table 1. Parameters obtained from the polarization curves for the different Al composites in the 3.5% NaCl solutions.

Sintering Temperature	Corrosion Parameter					
	$\beta_c/V \text{ dec}^{-1}$	E_{Corr}/V	$\beta_a/V \text{ dec}^{-1}$	$j_{\text{Corr}}/\mu\text{A cm}^{-2}$	$R_p/\Omega \text{ cm}^2$	$R_{\text{Corr}}/\text{mpy}$
900 °C	0.18	−0.855	0.22	7	478.3	0.0996
1100 °C	0.20	−0.830	0.23	9	664.5	0.0775
1300 °C	0.24	−0.965	0.195	27	155.9	0.3321

The CPP curve obtained for Al–TiC composite sintered at 900 °C (Figure 2, curve 1) shows a decrease of current with increasing potential in the less negative direction until the open-circuit potential (E_{Corr}) value was obtained at which the value of j_{Corr} is reached. This is due to the oxygen reduction that occurs on the surface of Al via the cathodic reactions that can be expressed by the following equations [9,26–28]:

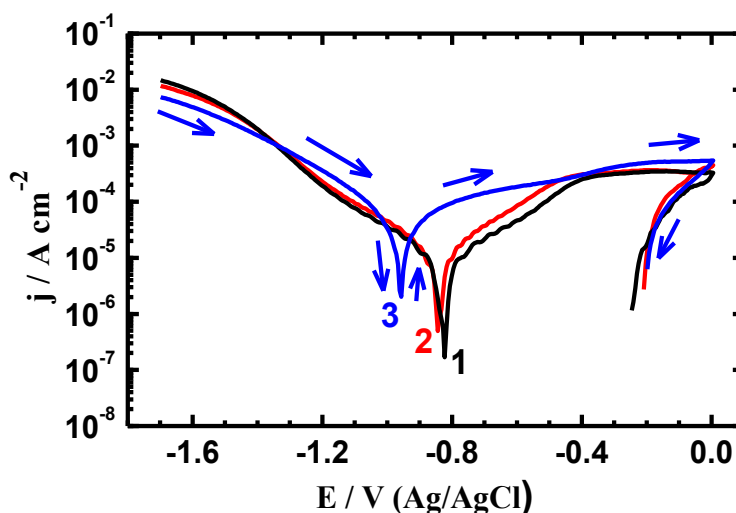
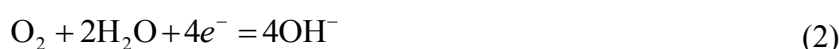


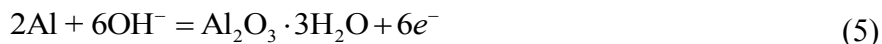
Figure 2. Cyclic potentiodynamic polarization curves obtained after 1 h immersion in 3.5% NaCl solutions for the Al–TiC composite sintered at (1) 900, (2) 1100, and (3) 1300 °C, respectively.

The consumed electrons in the cathodic reaction are produced from the anodic reaction in which the aluminum dissolves under the aggressiveness action of the chloride ions as well as the increase of potential values in the less negative direction as per the following reaction [9,11,26]:



In the early stages of the anodic branch, the aluminum surface develops an oxide film, which is indicated by the large passive region shown on the curve, this may be expressed as follows [9,11,26]:





The formed oxide layer gets destroyed with increasing the applied potential at the most negative values in the presence of the corrosive chloride species. This, in turn, leads to the dissolution of Al via the occurrence of uniform corrosion, as proven by the increase of current shown in Figure 2. This can be explained according to the following reaction [29,30]:



According to reaction (6), a salt barrier is formed within the pits on their formation, in this case AlCl_3 , which could then form AlCl_4^- and diffuses into the bulk of the solution. Another opinion claimed is that the chloride ions do not enter into the formed oxide layers but they are chemisorbed onto the oxide surface and act as a reaction partner, aiding the oxide to dissolve via the formation of oxychloride complexes, as per the following reaction [29,30]:



Increasing the temperature of sintering to 1100 °C (Figure 2, curve 2) led to increasing the cathodic, anodic, and corrosion (j_{Corr}) currents as well as the value of R_{Corr} , shifting E_{Corr} slightly to the more negative, and decreasing the value of R_p . The highest sintering temperature, 1300 °C (Figure 2, curve 3) raised the values of cathodic and anodic currents, j_{Corr} and R_{Corr} , while decreasing the value of R_p and shifted E_{Corr} further in the more negative direction with no indication on the occurrence of pitting corrosion. This was confirmed by the values of the corrosion parameters displayed in Table 1. The polarization results thus revealed that the best performance for the manufactured Al composite against corrosion in 3.5% NaCl solution was recognized to be for the sample sintered at 900 °C followed by the one at 1100 °C, while the worst resistance against corrosion was proven to be for the sample sintered at 1300 °C. This is due perhaps that the increase of sintering temperature increases the diffusion of Al metal and thus decreases the corrosion resistance of the composite's surface.

3.2. Chronoamperometric Measurements

In order to throw more light on the effect of sintering temperature on the pitting corrosion of the different manufactured Al composites, chronoamperometric current-time (CCT) curves were collected after 1 h immersion in 3.5% NaCl solutions followed by the application of a constant value of potential, $-0.1 \text{ V vs. Ag/AgCl}$ for another 1 h. Figure 3 shows CCT curves obtained in 3.5% NaCl solutions for the Al–TiC composites sintered at (1) 900, (2) 1100, and (3) 1300 °C, respectively. The lowest current is seen to be recorded for the composite that was sintered at 900 °C (Figure 3 curve 1), where the current initially decreased due to the presence of a preformed oxide film. Further decreases in the current with increasing time across the whole time of the experiment were recorded. This is because the composite at this condition does not corrode via pitting corrosion and also has a high corrosion resistance against uniform attack.

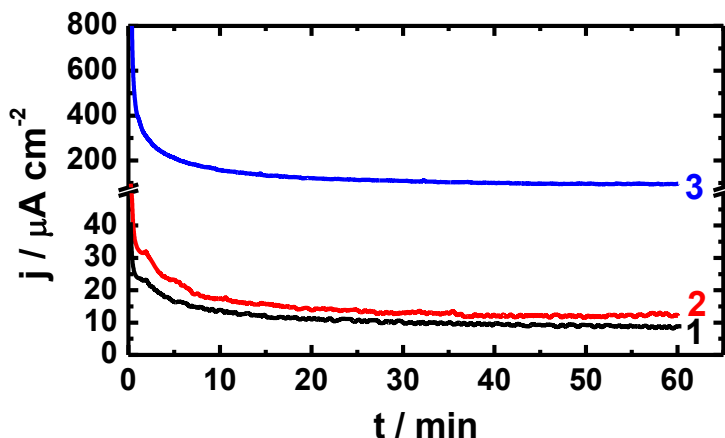


Figure 3. Potentiostatic current-time curves obtained at -100 mV for the Al-TiC composite sintered at (1) 900, (2) 1100, and (3) 1300 °C after 1 h immersion in 3.5% NaCl solutions.

Similar effects, but with slightly higher current values, were shown by sintering the Al-TiC composite at 1100 °C (Figure 3 curve 2). On the other hand, increasing the temperature of sintering to 1300 °C (Figure 3 curve 3) increased the absolute current values for the composite up on its immersion and over the time of the run to be much higher than those currents recorded for samples sintered at 900 and 1100 °C. This prevails that the composite that was sintered at 1300 °C suffers the highest general dissolution but no pitting corrosion occurs, as the current does not increase with time. The CCT data thus confirms the results obtained by CPP measurements that the best performance against corrosion was shown by the composite sintered at 900 °C, followed by the one sintered at 1100 °C.

3.3. Surface Morphology Investigations

In order to report the effect of sintering temperature on the surface morphology of the Al-TiC composite and whether pitting corrosion occurs after applying more active potential value, the scanning electron microscopy (SEM) investigations were carried out. Figure 4 shows the SEM micrographs obtained for Al-TiC composites sintered at (a) 900, (b) 1100, and (c) 1300 °C, respectively, after their immersion in 3.5% NaCl solutions for 1 h before applying -0.1 V vs. Ag/AgCl for another hour. The sample sintered at 900 °C (Figure 3a) depicts that its surface does not have any indications for the occurrence of pitting corrosion confirming its CCT behavior, where the current values were always decreasing with time as seen in Figure 3 (curve 1) [29,30]. Moreover, all other images taken for the composites sintered at 1100 and 1300 °C did not show any pits, but showed a corrosion attack towards the surface. The highest deterioration was evident for the Al sample sintered at 1300 °C, which may be due to the increased Al at the composite's surface. The SEM investigations are, thus, in good agreement with the data obtained by both CPP and CCT measurements.

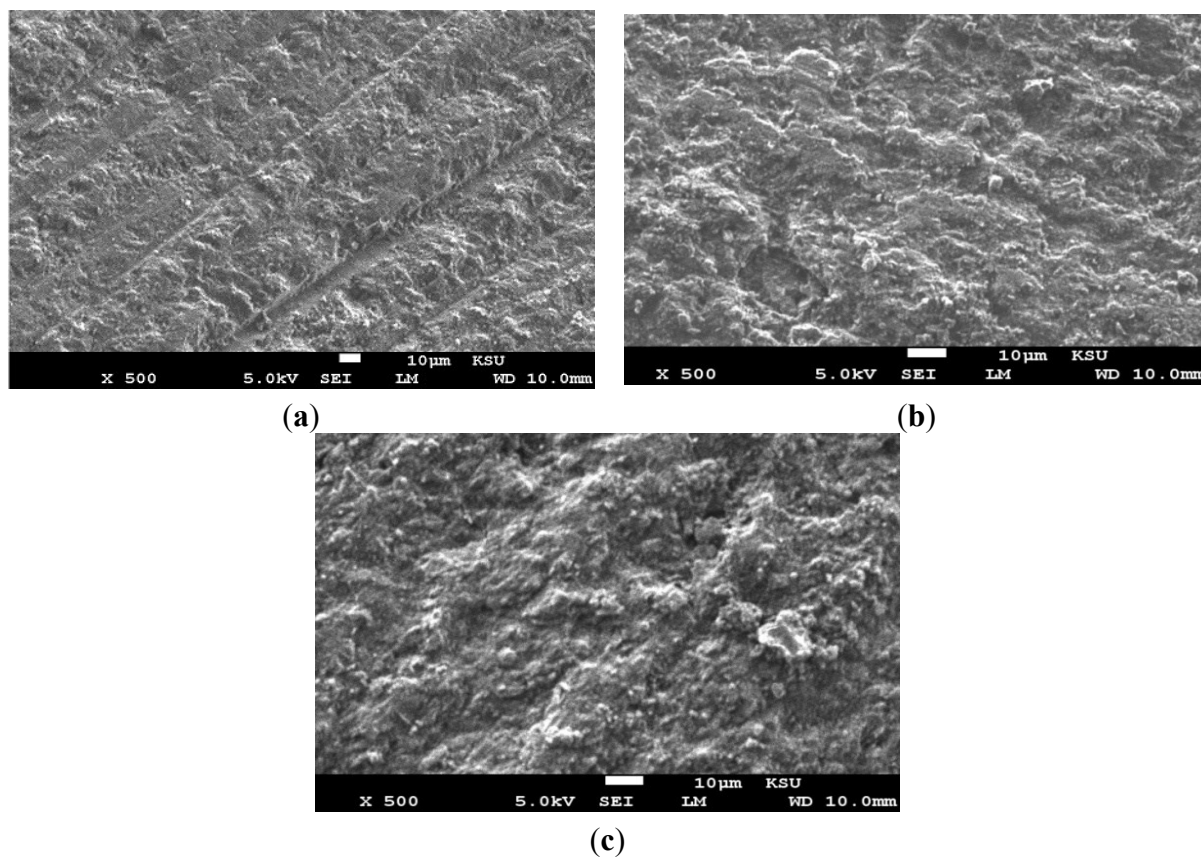


Figure 4. SEM images obtained for the surface of Al–TiC composite sintered at (a) 900, (b) 1100, and (c) 1300 °C after its immersion for 1 h in 3.5% NaCl solutions followed by applying a constant value of -0.1 V (Ag/AgCl) for another 1 h.

3.4. Open-Circuit Potential Measurements

The effect of increasing the sintering temperature on the free corrosion potential (open-circuit potential, OCP) of the Al–TiC composites was reported. The variation of the OCP of metals and composites with time usually gives valuable information on their corrosion phenomena. The variation of OCP with time (20 h) curves obtained for the Al–TiC composite sintered at (1) 900 °C, (2) 1100 °C, and (3) 1300 °C in 3.5% NaCl solutions are shown in Figure 5. It is clear from Figure 5 (curve 1) that the potential shifts rapidly at the early moments of immersion towards the negative direction as a result of the dissolution of a pre-immersion formed oxide layer. Then the potential shifts slightly to less negative values with time due to the equilibrium between the corrosion attack to the electrode surface and the formation of an oxide film on the surface. Increasing the sintering temperature (Figure 5, curve 2) greatly shifted the absolute potential of the composite to the less negative values from the first moment of electrode immersion and across the whole time of the experiment. This indicates that sintering the composite at 1100 °C increases its corrosion via dissolving the electrode surface by the chloride ion attack presented in the test solution. The highest sintering temperature, 1300 °C, as seen from the curve 3 of Figure 5 decreased the values of OCP in the negative direction with time, which indicates that the increase of temperature increases the corrosion of the fabricated composites. The results obtained from the change of the OCP with time thus confirm the data obtained by polarization

and chronoamperometric measurements that the corrosion resistance of the manufactured Al composites decreases according to their sintering temperature in the order of $900 > 1100 > 1300$ °C.

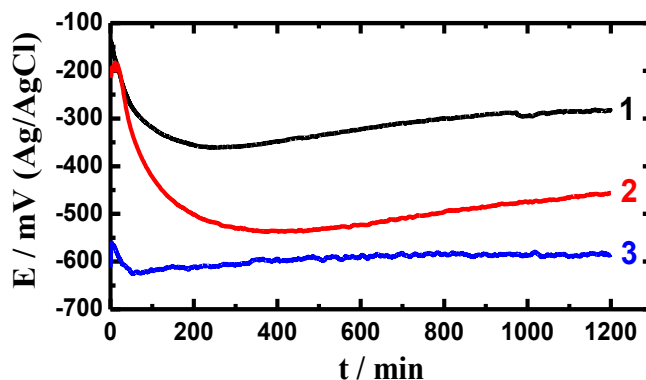


Figure 5. Change of the open circuit potential *versus* time curves obtained for the Al–TiC composite sintered at (1) 900, (2) 1100, and (3) 1300 °C in 3.5% NaCl solutions.

3.5. Electrochemical Impedance Spectroscopy (EIS)

Our EIS experiments were carried out to report the kinetic parameters for the composite/surface interface in the chloride test solution. Typical Nyquist plots obtained for the Al–TiC composite sintered at (1) 900, (2) 1100, and (3) 1300 °C after 1 h immersion in 3.5% NaCl solutions are shown respectively in Figure 6. The EIS plots were best fitted to the equivalent circuit shown in Figure 7. The values of the parameters obtained from fitting EIS data with the equivalent circuit depicted in Figure 7 are displayed in Table 2. According to universal convention, the symbols of the equivalent circuit are defined as following: R_s a solution resistance; Q constant phase elements (CPEs); R_{P1} a polarization resistance that represents the resistance between Al composite and a corrosion product layer; C_{dl} double layer capacitors; and R_{P2} a second polarization resistance for the corrosion product and solution interface.

The Nyquist plots of Figure 6 have only one semicircle for all Al composites after the different sintering temperatures, the bigger the diameter of the obtained semicircle the higher the corrosion resistance of the composite. The biggest diameter is seen for Al composite sintered at 900 °C followed by the one sintered at 1100 °C, but the smallest diameter was obtained for the sample sintered at 1300 °C. This behavior was also confirmed by the values of the parameters recorded in Table 2. Where the highest polarization (R_s , R_{P1} , and R_{P2}) values were assigned for the two composites sintered at 900 and 1100 °C, respectively. Also, the values of Q (CPEs) with their n values close to 0.5 represent Warburg impedance, which indicates that the corrosion of the Al composites does not take place via mass loss. The values of CPEs and also the values of C_{dl} were the smallest for 900 and 1100 °C, respectively and confirm that their corrosion was the lowest. The EIS data thus agree with the results obtained by polarization, chronoamperometry, and open-circuit potential that the composite fabricated at 900 °C has the best performance against corrosion in 3.5% NaCl solution.

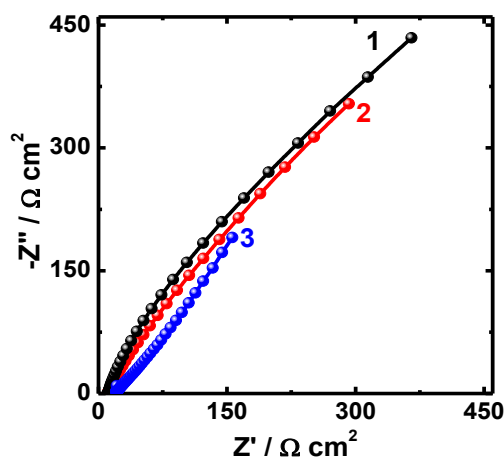


Figure 6. Typical Nyquist plots obtained for the Al–TiC composite sintered at (1) 900, (2) 1100, and (3) 1300 °C after 1 h immersion in 3.5% NaCl solutions.

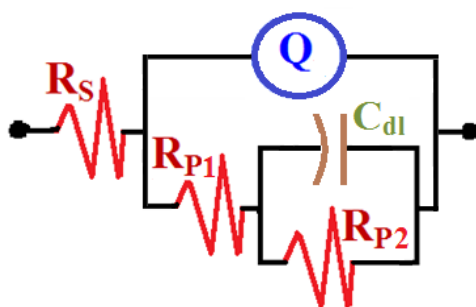


Figure 7. The equivalent circuit model used in the fitting of the obtained EIS data.

Table 2. Electrochemical impedance spectroscopy parameters obtained for the different Al composites in the electrolytic 3.5% NaCl test solution.

Sintering Temperature	Parameters					
	$R_s/\Omega \text{ cm}^2$	Q		$R_{P1}/\Omega \text{ cm}^2$	$C_{dl}/\text{F cm}^{-2}$	$R_{P2}/\Omega \text{ cm}^2$
		$Y_Q/\text{F cm}^{-2}$	n			
900 °C	16.09	0.002525	0.49	1.283	0.000381	545
1100 °C	15.48	0.002543	0.51	0.985	0.000524	419
1300 °C	13.97	0.007555	0.43	0.322	0.000145	243

4. Conclusions

In situ synthesizing of Al–TiC composites by HFIHF at sintering temperatures of 900, 1100, and 1300 °C was reported. The corrosion behavior of these composites in 3.5% NaCl solution was investigated using different electrochemical and surface analysis techniques. All measurements indicated that sintering the Al–TiC composite at a temperature of 900 °C presents the highest corrosion resistance by minimizing the values of j_{CORR} and R_{CORR} as well as increasing the value of R_P and preventing the occurrence of pitting corrosion. Manufacturing the composite at 1100 °C sintering temperature was found to also decrease the severity of corrosion through decreasing corrosion parameters against uniform and pitting attacks but the corrosion resistance of this composite was a bit lower than the composite sintered at 900 °C. The composite that was sintered at the highest

temperature, 1300 °C, showed the lowest resistance against uniform corrosion, although this composite did not suffer any pitting corrosion. Results together confirmed that the manufactured Al–TiC composites provided the best performance against corrosion at 900 °C followed by the samples fabricated at 1100 °C and the lowest resistance was obtained at 1300 °C.

Acknowledgments

This project was funded by the National Plan for Science, Technology and Innovation (MARRIFAH), King Abdulaziz City for Science and Technology, Kingdom of Saudi Arabia, Award Number (ADV-1853-2).

Author Contributions

E.-S. M. Sherif designed the work and conducting the corrosion experiments and wrote the manuscript. H. S. Abdo participated in the manufacturing and the corrosion tests for the composites. K. A. Khalil manufactured the composites. A. M. Nabawy designed the manufacturing of the samples.

Conflicts of Interest

The authors declare no conflict of interest.

References

1. Bockris, J.O.M.; Kang, Y. The protectivity of aluminum and its alloys with transition metals. *J. Solid State Electrochem.* **1997**, *1*, 17–35.
2. Sherif, E.-S.M.; Ammar, H.R.; Khalil, K.A. A comparative study on the electrochemical corrosion behavior of microcrystalline and nanocrystalline aluminum in natural seawater. *Int. J. Electrochem. Sci.* **2015**, *10*, 775–785.
3. Fogagnolo, J.B.; Velasco, F.; Robert, J.H.; Torralba, J.M. Effect of mechanical alloying on the morphology, microstructure and properties of aluminium matrix composite powders. *Mater. Sci. Eng. A* **2003**, *342*, 131–143.
4. Sherif, E.-S.M.; Ammar, H.R.; Khalil, K.A. Effects of copper and titanium on the corrosion behavior of newly fabricated nanocrystalline aluminum in natural seawater. *Appl. Surf. Sci.* **2014**, *301*, 142–148.
5. Despić, A.R.; Dražić, D.M.; Purenović, M.M.; Ciković, N. Electrochemical properties of aluminium alloys containing indium, gallium and thallium. *J. Appl. Electrochem.* **1976**, *6*, 527–542.
6. Sherif, E.-S.M. Electrochemical investigations on the corrosion inhibition of aluminum by 3-amino-1,2,4-triazole-5-thiol in naturally aerated stagnant seawater. *J. Ind. Eng. Chem.* **2013**, *19*, 1884–1889.
7. Sherif, E.-S.M. Corrosion and Corrosion Inhibition of Aluminum in Arabian Gulf Seawater and Sodium Chloride Solutions by 3-Amino-5-Mercapto-1,2,4-Triazole. *Int. J. Electrochem. Sci.* **2011**, *6*, 1479–1492.

8. Sherif, E.-S.M.; Almajid, A.A.; Latif, F.H.; Junaedi, H. Effects of Graphite on the Corrosion Behavior of Aluminum-Graphite Composite in Sodium Chloride Solutions. *Int. J. Electrochem. Sci.* **2011**, *6*, 1085–1099.
9. Latief, F.H.; Sherif, E.-S.M.; Almajid, A.A.; Junaedi, H. Fabrication of exfoliated graphite nanoplatelets-reinforced aluminum composites and evaluating their mechanical properties and corrosion behavior. *J. Anal. Appl. Pyrolysis* **2011**, *92*, 485–492.
10. Ambat, R.; Davenport, A.J.; Scamans, G.M.; Afseth, A. Effect of iron-containing intermetallic particles on the corrosion behaviour of aluminium. *Corros. Sci.* **2006**, *48*, 3455–3471.
11. Sherif, E.-S.M.; Soliman, M.S.; El-Danaf, E.A.; Almajid, A.A. Effect of Equal-Channel Angular Pressing Passes on the Corrosion Behavior of 1050 Aluminum Alloy in Natural Seawater. *Int. J. Electrochem. Sci.* **2012**, *7*, 2846–2859.
12. Sherif, E.-S.M.; El-Danaf, E.A.; Soliman, M.S.; Almajid, A.A. Corrosion Passivation in Natural Seawater of Aluminum Alloy 1050 Processed by Equal-Channel-Angular-Press. *Int. J. Electrochem. Sci.* **2013**, *8*, 1103–1116.
13. Sulka, G.D.; Parkoła, K.G. Temperature influence on well-ordered nanopore structures grown by anodization of aluminium in sulphuric acid. *Electrochim. Acta* **2007**, *52*, 1880–1888.
14. Zahariev, A.; Kanazirski, I.; Girginov, A. Anodic alumina films formed in sulfamic acid solution. *Inorg. Chim. Acta* **2008**, *361*, 1789–1792.
15. Belkhaouda, M.; Bazzi, L.; Salghi, R.; Jbara, O.; Benlhachmi, A.; Hammouti, B.; Douglad, J. Effect of the heat treatment on the behaviour of the corrosion and passivation of 3003 aluminium alloy in synthetic solution. *J. Mater. Environ. Sci.* **2010**, *1*, 25–33.
16. Adeosun, S.O.; Sekunowo, O.I.; Balgoun, S.A.; Obiekea, V.D. Corrosion Behaviour of Heat-Treated Aluminum-Magnesium Alloy in Chloride and EXCO Environments. *Int. J. Corros.* **2012**, doi:10.1155/2012/927380.
17. Chen, S.; Chen, K.; Peng, G.; Jia, L.; Dong, P. Effect of heat treatment on strength, exfoliation corrosion and electrochemical behavior of 7085 aluminum alloy. *Mater. Des.* **2012**, *35*, 93–98.
18. Chen, S.-Y.; Chen, K.-H.; Dong, P.-X.; Ye, S.-P.; Huang, L.-P. Effect of heat treatment on stress corrosion cracking, fracture toughness and strength of 7085 aluminum alloy. *Trans. Nonferrous Met. Soc. China* **2014**, *24*, 2320–2325.
19. El-Danaf, E.A. Mechanical properties and microstructure evolution of 1050 aluminum severely deformed by ECAP to 16 passes. *Mater. Sci. Eng. A* **2008**, *487*, 189–200.
20. Song, D.; Ma, A.B.; Jiang, J.; Lin, P.; Yang, D.; Fan, J. Corrosion behavior of equal-channel-angular-pressed pure magnesium in NaCl aqueous solution. *Corros. Sci.* **2010**, *52*, 481–490.
21. Zhang, J.; Zhang, K.-S.; Wu, H.-C.; Yu, M.-H. Experimental and numerical investigation on pure aluminum by ECAP. *Trans. Nonferrous Met. Soc. China* **2009**, *19*, 1303–1311.
22. Chung, M.-K.; Choi, Y.-K.; Kim, J.-G.; Kim, Y.-M.; Lee, J.-C. Effect of the number of ECAP pass time on the electrochemical properties of 1050 Al alloys. *Mater. Sci. Eng. A* **2004**, *366*, 282–291.
23. Furukawa, M.; Horita, Z.; Nemoto, M.; Langdon, T.G. Review: Processing of metals by equal-channel angular pressing. *J. Mater. Sci.* **2001**, *36*, 2835–2843.

24. Akiyama, E.; Zhang, Z.; Watanabe, Y.; Tsuzaki, K. Effects of severe plastic deformation on the corrosion behavior of aluminum alloys. *J. Solid State Electrochem.* **2009**, *13*, 277–282.
25. Fujda, M.; Kvačkaj, T.; Nagyová, K. Improvement of Mechanical Properties for EN AW 6082 Aluminium Alloy Using Equal-Channel Angular Pressing (ECAP) and Post-ECAP Aging. *J. Met. Mater. Miner.* **2008**, *18*, 81–87.
26. Sherif, E.-S.M. Effects of exposure time on the anodic dissolution of Monel-400 in aerated stagnant sodium chloride solutions. *J. Solid State Electrochem.* **2012**, *16*, 891–899.
27. Young, L. *Anodic Oxide Films*; Academic Press: New York, NY, USA, 1961; pp. 4–9.
28. El-Etre, A.Y. Inhibition of aluminum corrosion using *Opuntia* extract. *Corros. Sci.* **2003**, *45*, 2485–2495.
29. Sherif, E.-S.M.; Park, S.-M. Effects of 1,5-Naphthalenediol on Aluminum Corrosion as a Corrosion Inhibitor in 0.50 M NaCl. *J. Electrochem. Soc.* **2005**, *152*, B205–B211.
30. Sherif, E.-S.M.; Park, S.-M. Effects of 1,4-naphthoquinone on aluminum corrosion in 0.50 M sodium chloride solutions. *Electrochim. Acta* **2006**, *51*, 1313–1321.

© 2015 by the authors; licensee MDPI, Basel, Switzerland. This article is an open access article distributed under the terms and conditions of the Creative Commons Attribution license (<http://creativecommons.org/licenses/by/4.0/>).